Investigation on the influence of atomic potentials on the above threshold ionization*

Tian Yuan-Ye(田原野)[a], Li Su-Yu(李苏宇)[a], Wei Shan-Shan(魏珊珊)[a], Guo Fu-Ming(郭福明)[a], Zeng Si-Liang(曾思良)[b,c], Chen Ji-Gen(陈基根)[d], and Yang Yu-Jun(杨玉军)[a]†

[a] *Institute of Atomic and Molecular Physics, Jilin University, Changchun* 130012, *China*
[b] *Data Center for High Energy Density Physics, Institute of Applied Physics and Computational Mathematics, Beijing* 100088, *China*
[c] *Science and Technology Computation Physics Laboratory, Institute of Applied Physics and Computational Mathematics, Beijing* 100088, *China*
[d] *Department of Physics and Materials Engineering, Taizhou University, Taizhou* 318000, *China*

(Received 5 September 2013; revised manuscript received 8 November 2013; published online 25 March 2014)

We systematically investigate the influence of atomic potentials on the above-threshold ionization (ATI) spectra in one-dimensional (1D) cases and compare them with the three-dimensional (3D) case by numerically solving the time-dependent Schrödinger equation. It is found that the direct ionization plateau and the rescattering plateau of the ATI spectrum in the 3D case can be well reproduced by the 1D ATI spectra calculated from the supersolid-core potential and the soft-core potential, respectively. By analyzing the factors that affect the yield of the ATI spectrum, we propose a modified-potential with which we can reproduce the overall 3D ATI spectrum. In addition, the influence of the incident laser intensities and frequencies on the ATI spectra calculated from the proposed modified potential is studied.

Keywords: above threshold ionization, model potential, angular distribution of photoelectron

PACS: 32.80.Rm, 42.50.Hz **DOI:** 10.1088/1674-1056/23/5/053202

1. Introduction

With the rapid development of ultrashort laser pulse technology, research on the law of the interaction between laser and matter has been deepened gradually, and some high-order nonlinear effects have been observed, including the high-order harmonic generation (HHG),[1–4] non-sequential double ionization (NSDI),[5,6] above-threshold ionization (ATI),[7–9] and so on; therefore, a great amount of thorough and extensive research in this field has been carried out. The ATI has been deeply investigated in the past several decades, and it was found that there exist two plateaus on the ATI spectrum, which correspond to the direct ionization and the rescattering processes of the ionized electron.[10–14] The ATI spectrum can be used to detect the carrier envelope phase of the laser pulses[15,16] and the internal structure of the atom or molecule.[17,18]

Theoretically, the study on the ATI is mainly through the numerical solutions of the time-dependent Schrödinger equation (TDSE). To obtain an accurate result, one has to use a very large computational box to contain the overall information about the ionized electron. Thus, under the high intensity and long wavelength laser condition, the study of the ATI spectrum is a tough task. Usually, people adopt the one-dimensional (1D) model to replace the three-dimensional (3D) one when the incident laser is linear polarization. The reason is that, the computational cost largely increases as the dimension of the calculation increases, and the 1D result can also present the essential physical mechanism in the interaction between laser and atom. In this scheme, the profile of the atomic potential plays an important role in the accuracy of the result, thus some works concentrated on the influence of the atomic potential on the phenomena of strong field physics.[19,20] For example, Silaev *et al.*[20] investigated and compared the structures of HHG calculated from 1D and two-dimensional (2D) potentials with the 3D numerical result, and it was found that, for the structure of HHG, the numerical results calculated from the 1D and the 2D potentials exhibit similar structures in the corresponding harmonic spectra. In this work, we investigate the influence of the 1D model potentials on the ATI spectra.

In order to explore the effects of the model potential, we first numerically solve the TDSE in 1D and 3D, then compare the results from different 1D model potentials and the 3D atom, and analyze the influence of the atomic potentials on the different ATI plateaus. Finally, we propose a modified potential which can qualitatively reproduce the overall plateau of the 3D atom, and investigate the ATI spectra of the proposed atom under the action of laser pulses whose frequencies and peak intensities are different.

*Project supported by the National Basic Research Program of China (Grant No. 2013CB922200), the National Natural Science Foundation of China (Grant Nos. 11274141, 11034003, 11304116, 11274001, and 11247024), and the Jilin Provincial Research Foundation for Basic Research, China (Grant No. 20140101168JC).

†Corresponding author. E-mail: yangyj@jlu.edu.cn

© 2014 Chinese Physical Society and IOP Publishing Ltd

2. Theoretical method

The ATI spectrum of a system can be obtained by numerically solving the TDSE that describes the interaction between a model atom and an intense laser pulse. Under the dipole approximation, in the velocity gauge, the TDSE of an atom under the action of an intense laser pulse is given by (atomic units are used throughout unless otherwise stated)

$$\mathrm{i}\frac{\partial}{\partial t}\psi(r,t)=\left[\frac{\hat{p}^2}{2}+\frac{1}{c}A(t)\cdot\hat{p}+V(r)\right]\psi(r,t), \tag{1}$$

where c is the speed of light in a vacuum, $A(t)$ denotes the vector potential of the laser field, $\hat{p}=-\mathrm{i}\nabla$ refers to the momentum operator, and $V(r)$ accounts for the potential function of the atom, which is the Coulomb potential in the 3D case. While in the 1D cases, there are five potential functions (i.e., soft-core, solid-core, pliant-core, supersolid-core, and modified potentials) describing the model atom, and they can be described by a general expression[18]

$$V_{1\mathrm{D}}(x)=-\frac{1}{(|x|^m+n)^{1/m}}, \tag{2}$$

where the values of m and n in the potential function are shown in Table 1. In this case, it can ensure that the calculated ionization energy of the model atom is 0.5 a.u. (the ground state energy of a hydrogen atom). In Table 1, we also present the energy of the first excited state for different potential functions. Using the Crank–Nicholson difference scheme, we numerically solve Eq. (1) and obtain the time-dependent wave function of the system at any moment.[21] Adopting the calculation scheme of Javanainen *et al.*,[22] we firstly calculate the continuous state wave function of the system, then project it onto the time-dependent wave function at the end of the laser pulse, and eventually calculate the ATI spectrum.

Table 1. Energy of the first excited state calculated from different potential functions.

Potential function	Soft-core	Solid-core	Pliant-core	Supersolid-core	Modified	H atom
(m,n)	(2.00, 2.00)	(1.00, 1.00)	(1.50, 1.45)	(0.50, 0.60)	(1.75,1.70)	–
Energy	–0.2329	–0.1804	–0.2135	–0.1163	–0.2247	–0.1250

In order to analyze the influence of the ionization probability on the ATI spectra, we also calculate the bound state wave functions and project them onto the time-dependent wave function, thus obtaining the population amplitude of the bound state at any moment

$$b_n(t)=\langle\varphi_n(x)/\psi(x,t)\rangle\,. \tag{3}$$

Then the ionization probability of the system can be obtained as

$$p_{\mathrm{ion}}=1-\sum_{n=0}^{N_{\max}}|b_n(t)|^2. \tag{4}$$

While in the 3D case, the wave function in the momentum space can be obtained from the wave function in the coordinate space through the Fourier transformation

$$\Phi(k,t)=\frac{1}{(2\pi)^{3/2}}\int\psi(r,t)\exp(-\mathrm{i}k\cdot r)\,\mathrm{d}r. \tag{5}$$

Substituting Eq. (5) into Eq. (1), we can obtain the TDSE in the momentum space. This equation can be solved by the time-dependent generalized pseudospectral scheme.[23] Using the calculated time-dependent wave function of the system, we calculate the information about the ATI utilizing the scheme proposed by Dionissopoulou *et al.*[24] At the end of the laser pulse, we can obtain the population of each state by projecting the eigen-state wave function in the field-free case onto the final-state wave function. By projecting the scattered continuum state

$$\Psi^-=4\pi\sqrt{\frac{\pi}{2k}}\sum_l\sum_{m=-l}^{l}\mathrm{i}^l\,\mathrm{e}^{-\mathrm{i}\delta_l}\mathrm{Y}^*_{lm}(\boldsymbol{k})\mathrm{Y}_{lm}(\boldsymbol{r})R_{kl}(r) \tag{6}$$

onto the wave function at the end of the laser pulse, if $c_l(\varepsilon,t)$ is the population amplitude of the normalized continuum state, the angular distribution of photoelectrons can be obtained as

$$\frac{\mathrm{d}^2P_\varepsilon(\boldsymbol{k},t)}{\mathrm{d}\boldsymbol{k}\,\mathrm{d}\varepsilon}=\left|\sum_l\sum_{m=-l}^{l}(-\mathrm{i})^l\,\mathrm{e}^{\mathrm{i}\delta_l}\mathrm{Y}_{lm}(\boldsymbol{k})c_l(\varepsilon,t)\right|^2. \tag{7}$$

For the case of a linearly polarized laser pulse, it can be reduced to

$$\frac{\mathrm{d}^2P_\varepsilon(\vartheta,t)}{\mathrm{d}\vartheta\,\mathrm{d}\varepsilon}=\left|\sum_l(-\mathrm{i})^l\,\mathrm{e}^{\mathrm{i}\delta_l}\mathrm{Y}_{l0}(\vartheta)c_l(\varepsilon,t)\right|^2. \tag{8}$$

For the 3D case, if one knows the probability amplitude $c_l(\varepsilon)$ of the continuum state whose energy is ε and partial is l, then one can obtain the single differential cross section

$$\frac{\mathrm{d}P_\varepsilon}{\mathrm{d}\varepsilon}=\sum_l|c_l(\varepsilon)|^2. \tag{9}$$

The photoelectron energy–angular distribution can be calculated by the double differential cross section

$$\frac{\partial^2P}{\partial E\sin\theta\partial\theta}=2\pi\left(\frac{\partial^3P}{\partial E\partial\Omega}\right). \tag{10}$$

In order to compare with the 1D result, we calculate the ATI spectrum in the direction of the laser electric field and name it the axial ATI spectrum in this paper. Here, the axial ATI spectrum is defined as the number of photoelectrons that can be obtained in a given energy range by integrating the momentum in the direction perpendicular to that of the laser field. As for the measurement of the ATI spectrum of the high energy electron, the collection angle should be chosen to be a very small angle, which should be 3°–5°. However, in our calculation, the momentum is chosen in a 2D plane, and in this plane, we integrate the momentum in the direction perpendicular to that of the electric field, and the range of momentum integration is set from 0 a.u. to 0.866 a.u. (in effect, the result will be close to the axial one if a small range of integration is used, however, in order to reduce the jitter of the curve of the ATI spectrum, we choose the above range) corresponding to the energy range from 0 a.u. to 0.375 a.u. The linearly polarized laser pulse is selected to have a Gaussian shape, and its electric field is

$$E(t) = E_0 \exp\left(-4\ln 2\frac{t^2}{\tau_p^2}\right)\sin(\omega t), \tag{11}$$

where E_0 and ω are the peak amplitude and the central frequency of the laser pulse, respectively. Here, $\tau_p = \pi N_p/\omega$ is the full width at half maximum (FWHM) of the laser pulse, $N_p = 5$ refers to the number of the optical cycles and is used throughout this paper.

3. Results and discussion

In the 1D case, Silaev *et al.*[20] chose four kinds of potential functions, i.e., soft-core potential, solid-core potential, pliant-core potential, and supersolid-core potential, to describe the model atom, whose general expression is given by Eq. (2). In Fig. 1(a), we present the ATI spectra of these model atoms irradiated by an ultrashort laser pulse, whose peak amplitude of the electric field and central wavelength are E_0 =0.067 and 800 nm, respectively, and the corresponding Keldysh parameter[25] $\gamma = \sqrt{I_p/(2U_p)}$ is 0.85. It can be seen from the figure that there are two plateaus in the ATI: one ends at $2U_p$ and the other ends at $10U_p$, where $U_p = E_0^2/4/\omega^2$ is the pondermotive energy of the laser pulse. The lower energy plateau has a higher intensity, and is generated from the direct ionization of the atom. The high energy plateau has a lower intensity, and is generated from the rescattering of the ionized electron. For the cutoff energy of the ATI spectra, these atomic potentials are almost the same. Large derivations present in the intensities of the ATI spectra calculated from the four atomic potentials.

For the purpose of comparison, we calculate the 3D and the corresponding axial ATI spectra, and find that they both exhibit the two plateaus. Under the action of a low frequency linearly polarized laser pulse, the main population of ATI lies in the direction of the laser electric field (axial direction), and many experiments only collect the ionized electrons in the axial direction, thus we also present the axial ATI spectra in Fig. 1. We can see from Fig. 1(a) that the 1D and the 3D ATI spectra have the same energy cutoffs, i.e., $2U_p$ and $10U_p$; however, there exists a difference between them, the yields are different. It can be seen from Fig. 1(b) that at a shorter distance (near the nuclear zone), the potential well is deep, the supersolid-core potential is closer to the exact one, while at a longer distance (far away from the nuclear zone), the soft-core potential is much closer to the exact one. Therefore we can say that, for the overall structure of the ATI spectra, the 1D results are not completely identical to the 3D one. However, the 1D ATI spectra are qualitatively analogous to the 3D axial one. The results show that the non-axial population also plays an important role under this laser condition.

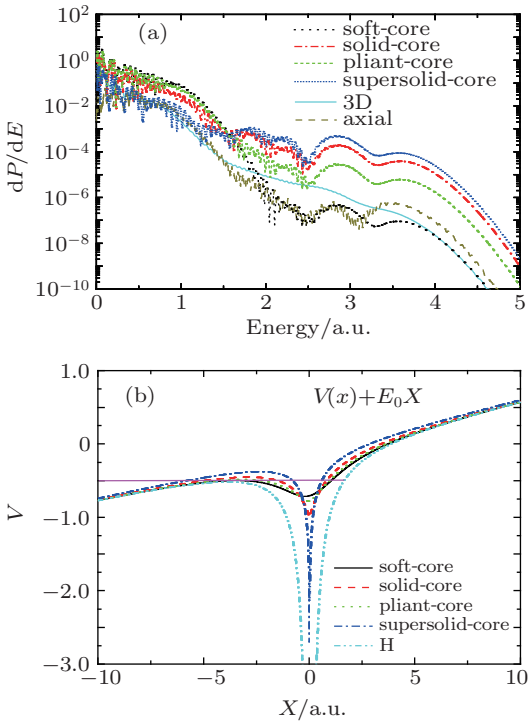


Fig. 1. (color online) (a) ATI spectra of the model atom calculated from the 3D potential function and different 1D potential functions, (b) model potential functions under the action of a laser field, where the magenta curve denotes the ground state energy of the system.

In order to obtain a result which qualitatively agrees with the 3D axial one using an adaptive 1D model potential, we separately analyze the ATI spectra in high energy and low energy. In low energy, it is found that the intensity profiles of the low energy plateau in the 1D ATI spectra calculated from soft-core potential (dotted black curve), pliant-core potential (short-dashed green curve), and solid-core potential (dash-dotted red curve) are in good agreement with each other, while

the result from the solid-core potential (dash-dotted red curve) is lower in intensity compared to that from the other two. The 1D ATI spectrum calculated from the supersolid-core potential has a much lower intensity compared to the three former ones, and its structure is quite different from that of the three former ones. There exists a big difference between the 1D ATI spectra in these cases and the axial ATI spectrum, and only the ATI spectrum calculated from the supersolid-core potential is identical to the axial ATI spectrum in intensity.

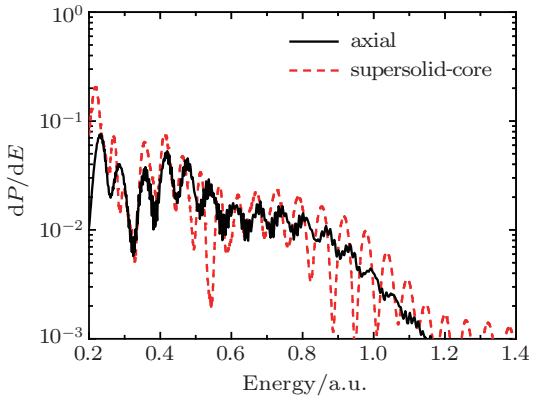


Fig. 2. (color online) Low energy plateaus of the axial and the 1D ATI spectra of the model atom.

In order to find out the causes of the above phenomena, i.e., under the same incident laser, a distinct difference exists between the low energy plateaus of the ATI spectra calculated from different potential functions, we analyze the classical three-step model.[26] In the ionization stage, there exists a big difference in the potential barriers consisting of the laser field and different atomic potentials. Though under the action of the same laser pulse, the potential barrier which the electron will penetrate widens and heightens gradually and from the soft-core potential, the pliant-core potential, the solid-core potential, and the supersolid-core potential to the actual Coulomb potential of the hydrogen atom, leading to the gradual decrease of the ionization probability. To verify this conclusion, we calculate the change of the ionization of the atom with time in the intense laser field according to Eq. (4) and show it in Fig. 3. The parameters of the laser pulse are the same as those adopted in the previous part. It can be seen from Fig. 3 that the ionization probabilities calculated from the supersolid-core potential, the solid-core potential, the pliant-core potential, and the soft-core potential increase in sequence. Particularly, the ionization probability calculated from the supersolid-core potential is closer to the 3D result, which can be attributed to the fact that the structure of the supersolid-core potential is closer to that of the actual Coulomb potential of the H atom. In order to verify this conclusion, we calculate the energy of the first excited state in different model potentials. Obviously, we can see from Table 1 that the energy of the first excited state calculated from the supersolid-core potential is also close to that of the H atom. We can arrive at the same conclusion by calculating the probability of ionization and the energy of the first excited state. The ionized electron will move in the laser field after ionization, and get out of the potential well at the same time for different potential functions due to the same incident laser field; as a result, the generated effects like dispersion are in agreement and the influence of this process on the atom is the same for different potential functions. The low energy plateau of the ATI spectrum comes from the direct ionization, therefore, in the low energy region, the 3D ATI spectrum of the H atom can be replaced by the 1D result from the supersolid-core potential, which can be clearly seen in Fig. 2.

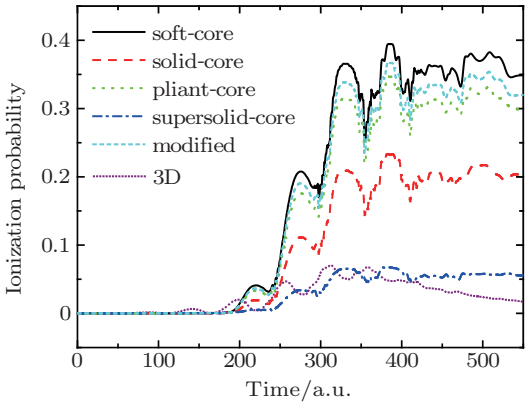


Fig. 3. (color online) Time evolution of the ionization probability calculated from different potential functions.

As for the high energy plateau (i.e. the rescattering plateau), the intensities of the axial ATI spectrum and the ATI spectra calculated from the soft-core potential, the pliant-core potential, the solid-core potential, and the supersolid-core potential increase gradually and only the 1D ATI spectrum from the soft-core potential is close to the axial one (see Fig. 1). The elastic cross section of the soft-core potential is much smaller than that of the other potential functions,[8] which can be attributed to the fact that the change of the soft-core potential is slower than that of the other potentials and the force acted on the atom is smaller. As a result, for the soft-core potential, the electron has less opportunity to be scattered elastically compared to the solid-core potential, the pliant-core potential, and the supersolid-core potential. Therefore, in the case that the ionization probability is the same, the intensity of the ATI spectrum in the rescattering plateau corresponding to the soft-core potential is lower than that corresponding to the pliant-core potential, the solid-core potential, and the supersolid-core potential, and is in agreement with that of the 3D H atom. For this reason, in the high energy region of the ATI spectrum, the 3D result of the H atom can be replaced by the 1D one from the soft-core potential.

Through the analysis of low energy and high energy plateaus, we find that there is no 1D ATI spectrum calculated from the potential functions given in Fig. 1 that can fit well the overall axial and 3D ATI spectra, and only the 1D ATI spectrum calculated from the pliant-core potential is relatively close to the axial one. For this reason, we need to build a potential function with which we can obtain the ATI spectrum closer to the overall axial one, thus investigating the 3D ATI spectrum through the 1D one. Here, we choose the same parameters as those in Fig. 1, and build a modified function (its expression is given in Eq. (2) and the corresponding values of m and n are shown in Table 1) through which we can use the obtained 1D result to investigate the overall structure of the axial ATI spectrum. As shown in Fig. 4, the 1D ATI spectrum calculated from the modified potential is much closer to the overall axial one compared to that calculated from the pliant-core potential, and the main difference is that its intensity is one order of magnitude larger than that of the axial result. As has been discussed above, we can utilize the 1D ATI spectrum obtained from the modified function to replace the overall 3D one in calculation, thereby greatly reducing the computational time.

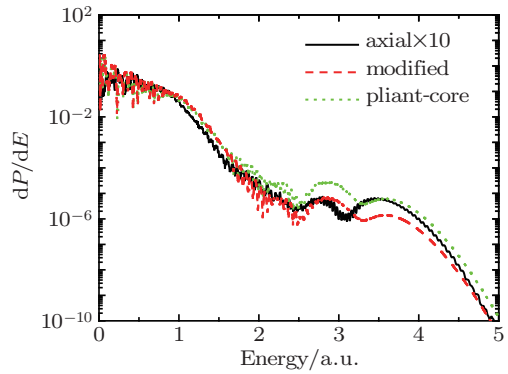


Fig. 4. (color online) Axial ATI spectrum and the 1D ones of the model atom calculated from the modified potential and the pliant-core potential.

Figure 5 shows the 1D and the axial ATI spectra in different laser fields: (a) $E_0 = 0.0713$, (b) $E_0 = 0.0671$, (c) $E_0 = 0.0633$, and (d) $E_0 = 0.0475$, and the wavelength is still 800 nm. The corresponding Keldysh parameters are 0.80, 0.85, 0.90, and 1.20, which transit from the tunneling regime to the multiphoton one. It can be seen from the figure that at different intensities, the overall structure of the 1D ATI spectrum calculated from the modified potential is still in good agreement with that of the axial one, and they are more identical to each other in the tunneling regime. Hence, we can use the modified potential to investigate the 1D and the 3D ATI spectra at different incident intensities.

Can the 3D ATI spectrum be reproduced by the modified potential we built when the frequency of the laser pulse changes? In the following, we investigate this issue. Here, the frequencies of the laser pulses are chosen as (a) $\omega_0 = 0.057$, (b) $\omega_0 = 0.114$, (c) $\omega_0 = 0.228$, and (d) $\omega_0 = 1$, and we adjust their intensities to ensure that the corresponding Keldysh parameters are 0.85. Figure 6 shows the 1D ATI spectrum calculated from the modified potential and the axial one of the hydrogen atom. It can be seen from the figure that the 1D and the axial ATI spectra are still in agreement with each other, however a difference in the structure appears as the frequency increases.

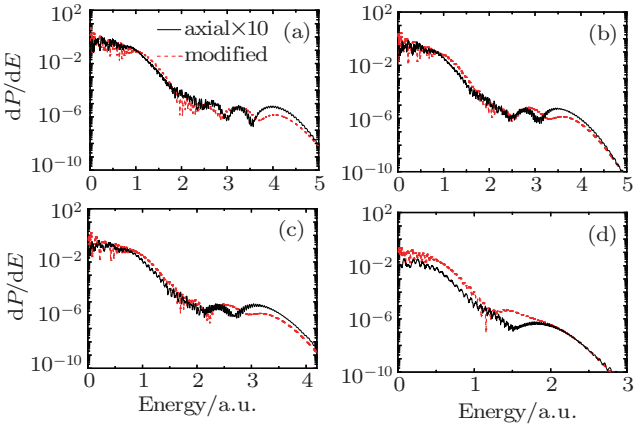


Fig. 5. (color online) Axial ATI spectra and the 1D ones from the modified potential at different incident intensities, the corresponding electric field strengths are (a) $E_0 = 0.0713$, (b) $E_0 = 0.0671$, (c) $E_0 = 0.0633$, and (d) $E_0 = 0.0475$.

As for the difference in the structures of 1D and axial ATI spectra shown in Fig. 6, we can analyze from the perspective of the photoelectron energy–angular distribution, as shown in Fig. 7. It can be known from the definition of the transverse momentum that the transverse momentum is the component of the momentum which is perpendicular to the polarization direction of the electric field. In the results of our 3D calculation, for the low frequency case, the transverse momentum is very small; whereas, for the high frequency case, the effect of the transverse momentum is distinct, which can be clearly seen from Fig. 7. For this reason, we can say that the result comes from the influence of the transverse momentum. Under the action of a high frequency laser pulse, the photoelectron energy–angular distribution displays complex interference patterns, which consist of a series of rings (see Fig. 7(b)). The rings represent the angular distribution of the photoelectron, which indicates that the photoelectron emission is almost independent of the direction. As has been stated in the theoretical method part, the axial ATI spectrum contains only the component in the direction parallel with the electric field, and the non-axial component is not included, as a result, there exists a difference between the axial ATI spectrum and the ATI spectrum that contains all the information about the ATI process. However, the peak structure of the ATI spectrum can still be described by the axial ATI spectrum, as shown in

Fig. 6(d). Under the action of a low frequency laser pulse, we can see that the intensity of the photoelectron emission in the direction parallel with the electric field of the incident laser pulse is much larger than that in other directions (see Fig. 7(a)). Therefore, we can say that in the low frequency laser field, the axial component basically contains the information about the ATI process, which has already been observed in the experiments.[27] Consequently, under the action of a low frequency laser pulse, the ATI spectrum can be accurately described by its axial component.

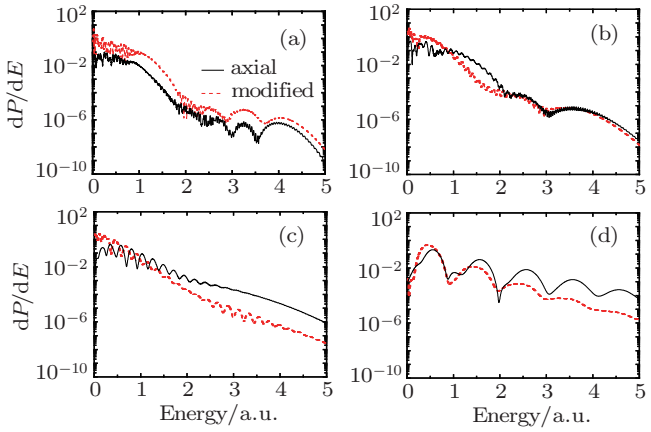


Fig. 6. (color online) Axial ATI spectra and the 1D ones calculated from the modified potential under the laser pulses whose frequencies are (a) $\omega_0 = 0.057$, (b) $\omega_0 = 0.114$, (c) $\omega_0 = 0.228$, and (d) $\omega_0 = 1$.

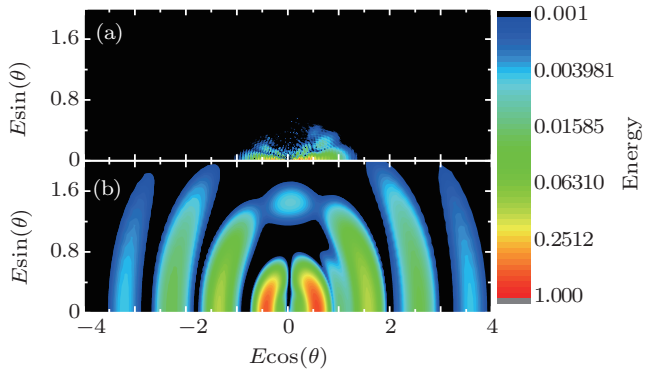


Fig. 7. (color online) Energy–angular distribution of the photoelectron at the frequencies of (a) 0.057 and (b) 1, where the pulse duration of the incident laser is five optical cycles. The laser field amplitudes are (a) E_0 =0.067 and (b) E_0 =1.176.

4. Conclusion

In this paper, we systematically investigate and compare the ATI spectra in 1D and 3D cases by numerically solving the TDSE that describes the interaction between the model atom and the ultrashort laser pulse. It is found that, under the action of a low frequency laser pulse, we fail to obtain the accurate 1D ATI spectra that are identical to the 3D results by utilizing the existing potentials. However, the 1D ATI spectra calculated from the supersolid-core potential and the soft-core potential can reproduce the direct ionization plateau and the rescattering plateau of the 3D ATI spectrum, respectively. By analyzing the ionization probability, the energy of the first excited state, and the rescattering cross section, we verify the conclusion that the direct ionization plateau and the rescattering plateau of the ATI spectrum depend on the energies of the first excited state and the rescattering cross section, respectively. By adjusting the two factors that affect the structure of the ATI spectrum, we build a modified potential which can reproduce the overall 3D ATI spectrum. In addition, under the action of the incident laser with different intensities and frequencies, the 3D result can still be well reproduced by the modified potential in the 1D case.

Acknowledgment

We acknowledge the High Performance Computing Center of Jilin University for their supercomputer support.

References

[1] Li X F, L'Huillier A, Ferray M, Lompré L A and Mainfray G 1989 *Phys. Rev. A* **39** 5751
[2] Macklin J J, Kmetec J D and Gordon C L 1993 *Phys. Rev. Lett.* **70** 766
[3] Wang B B, Li X F and Fu P M 1998 *Chin. Phys. Lett.* **15** 195
[4] Luo L Y, Du H C and Hu B T 2012 *Chin. Phys. B* **21** 033202
[5] Fittinghoff D N, Bolton P R, Chang B and Kulander K C 1992 *Phys. Rev. Lett.* **69** 2642
[6] Walker B, Sheehy B, DiMauro L F, Agostini P, Schafer K J and Kulander K C 1994 *Phys. Rev. Lett.* **73** 1227
[7] Agostini P, Fabre F, Mainfray G, Petite G and Rahman N K 1979 *Phys. Rev. Lett.* **42** 1127
[8] Tian Y Y, Guo F M and Yang Y J 2013 *Acta Phys. Sin.* **62** 073202 (in Chinese)
[9] Sun C P, Zhao S F, Chen J H and Zhou X X 2011 *Chin. Phys. B* **20** 113201
[10] Cormier E, Garzella D, Breger P, Agostini P, Chériaux G and Leblanc C 2001 *J. Phys. B* **34** L9
[11] Becker W, Grasbon F, Kopold R, Milosevic D B, Paulus G G and Walther H 2002 *Advances in Atomic, Molecular, and Optical Physics* **48** 35
[12] Armstrong G S J, Parker J S and Taylor K T 2011 *New J. Phys.* **13** 013024
[13] Toyota K, Tolstikhin O I, Morishita T and Watanabe S 2009 *Phys. Rev. Lett.* **103** 153003
[14] Li M, Liu Y Q, Liu H, Ning Q C, Fu L B, Liu J, Deng Y K, Wu C Y, Peng L Y and Gong Q H 2013 *Phys. Rev. Lett.* **111** 023006
[15] Tong X M, Hino K and Toshima N 2006 *Phys. Rev. A* **74** 031405
[16] Kling M F, Rauschenberger J, Verhoef A J, Hasovic E, Uphues T, Milošević D B, Muller H G and Vrakking M J J 2008 *New J. Phys.* **10** 025024
[17] Meckel M, Comtois D, Zeidler D, Staudte A, Pavičić D, Bandulet H C, Pépin H, Kieffer J C, Dörner R, Villeneuve D M and Corkum P B 2008 *Science* **320** 1478
[18] van der Zwan E V and Lein M 2012 *Phys. Rev. Lett.* **108** 043004
[19] Su Q and Eberly J H 1991 *Phys. Rev. A* **44** 5997
[20] Silaev A A, Ryabikin M Y and Vvedenskii N V 2010 *Phys. Rev. A* **82** 033416
[21] Yang Y J, Chen G, Chen J G and Zhu Q R 2004 *Chin. Phys. Lett.* **21** 652
[22] Javanainen J, Eberly J H and Su Q 1988 *Phys. Rev. A* **38** 3430
[23] Zhou Z Y and Chu S I 2011 *Phys. Rev. A* **83** 013405
[24] Dionissopoulou S, Mercouris T, Lyras A and Nicolaides C A 1997 *Phys. Rev. A* **55** 4397
[25] Sprangle P, Peñano J R and Hafizi B 2002 *Phys. Rev. E* **66** 046418
[26] Corkum P B 1993 *Phys. Rev. Lett.* **71** 1994
[27] Ray D, Ulrich B, Bocharova I, Maharjan C, Ranitovic P, Gramkow B, Magrakvelidze M, De S, Litvinyuk I V, Le A T, Morishita T, Lin C D, Paulus G G and Cocke C L 2008 *Phys. Rev. Lett.* **100** 143002